232213

UCRL-JC-126818
PREPRINT

High-Energy X-ray Microscopy of Laser-Fusion Plasmas at the National Ignition Facility

J. A. Koch, O. L. Landen, B. A. Hammel,
J. Seely, T. W. Barbee, Jr., G. Bennet,
C. Brown, P. Celliers, L. B. Da Silva,
S. G. Glendinning, W. Hsing, D. H. Kalantar

This paper was prepared for and presented to the
9th National Topical Conference on High Temperature Plasma Diagnostics
St. Petersburg, Russia
June 2-4, 1997

August 26, 1997

Lawrence Livermore National Laboratory

High-Energy X-ray Microscopy of Laser-Fusion Plasmas at the National Ignition Facility

J. A. Koch, O. L. Landen, B. A. Hammel, J. Seely[a], T. W. Barbee, Jr., G. Bennet[b], C. Brown[a], P. Celliers, L. B. Da Silva, S. G. Glendinning, W. Hsing[b], D. H. Kalantar

Lawrence Livermore National Laboratory, P. O. Box 808, L-473, Livermore CA, U.S.A. 94550
[a]Naval Research Laboratory, Washington DC, U.S.A. 20375
[b]Los Alamos National Laboratory, Los Alamos NM, U.S.A. 87545

Abstract - Multi-keV x-ray microscopy will be an important laser-produced plasma diagnostic at future megajoule facilities such as the National Ignition Facility (NIF). In preparation for the construction of this facility, we have investigated several instrumentation options in detail, and we conclude that near normal incidence single spherical or toroidal crystals may offer the best general solution for high-energy x-ray microscopy at NIF and at similar large facilities. Kirkpatrick-Baez microscopes using multi-layer mirrors may also be good secondary options, particularly if apertures are used to increase the band-width limited field of view.

X-ray microscopy has made numerous critical contributions to the current state of knowledge in inertial confinement fusion (ICF) research [1] and in other areas of laser-produced plasma research, and is expected to continue to be vital for experiments at the 1.6 MJ National Ignition Facility (NIF) under construction at Lawrence Livermore National Laboratory (LLNL). Detector-mounted pinholes and slits are typically used in current experiments at LLNL and at other facilities; however, the extreme environment at NIF implies that there will be an exclusion zone with a radius of ~ 200 mm, inside of which pinholes and associated shielding on the detector may not survive high-energy experiments. This distance is further than desired for pinhole imaging due to diffractive degradation of spatial resolution and due to decreased collection solid angles.

In anticipation of experiments at NIF, we have begun a systematic investigation of various options for x-ray imaging at energies of ~ 4 - 13 keV. X-ray sources in this spectral region are generally line emitters, and this implies that high efficiency is needed only over a relatively narrow spectral region containing the emission line of interest. However, various emission lines at different energies are of interest, and this implies that quasi-monochromatic x-ray imaging instruments should have a flexible operating energy. Finally, typical imaging requirements are 2 - 10 μm spatial resolution over 0.5 - 2 mm fields of view in one or two dimensions.

The options being considered fall into two categories. The first category is short working-distance, expendable imaging elements, and includes primarily pinholes and their one-dimensional analog, slits. The second category is long working-distance, reusable diagnostics which are designed to survive high-energy experiments, and this category includes primarily reflective-optic imaging systems. Types of imaging systems being considered include metal-mirror Kirkpatrick-Baez (KB) microscopes [2], multi-layer coated mirror KB microscopes, bent-crystal KB microscopes, and single spherical [3] or toroidal [4] crystal microscopes. Our current strategy is to investigate close working-distance, target-mounted pinholes in Nova experiments while simultaneously investigating reflective optic imaging systems for long-term implementation at NIF.

The image exposure (e.g. in W/cm^2) obtained on a detector by an imaging system can be written generally as $(\Omega\eta/M_v M_h)I_0$, where I_0 is the spectrally integrated source brightness (e.g. in W/cm^2*Sr), M_v and M_h are the vertical and horizontal magnifications, Ω is the collection solid angle, and η is the collection efficiency including any losses due to reflectivity or band-width limitations. The scaled image brightness $\Omega\eta/M_vM_h$ (units of Sr), achievable while meeting a specified requirement for source spatial resolution over a given field of view, therefore serves as a figure-of-merit with which to weigh the various options. In a separate paper, we have investigated the achievable image brightness for several of the simplest options in various configurations [5] using analytical derivations and numerical ray-tracing. In this paper, we present some of the results for two-dimensional imaging near 6 keV with the Mn K-α (E = 5.9 keV, $\lambda/\Delta\lambda$ = 200) and the Mn He-α (E = 6.15 keV, $\lambda/\Delta\lambda \approx$ 2000), comparing the achievable image brightness for an Ir mirror KB; a multi-layer mirror KB [6]; a depth-graded multi-layer mirror KB [6]; a bent-crystal KB using mica in 3rd order [7], Si (220) [8], LiF (220) [8], and Si (422) [8]; and a spherical crystal using Si (422) [8], CaF_2 (111) in 3rd order [7] and quartz 22$\underline{4}$3 [9]. In Figs. 1 and 2 we plot the estimated image brightness for the Mn K-α source and the Mn He-α source, respectively, assuming a 200 mm source/optic distance and a magnification M = 4, while maintaining a spatial resolution better than 10 μm throughout a 2 mm field of view. For comparison, we also plot the estimated image brightness for a 8 μm-diameter pinhole operating at M = 4 with a detector distance of 200 mm. Those instruments which are not capable of achieving the 2 mm field of view due to reflector or source band-width limits are shows as open circles or triangles.

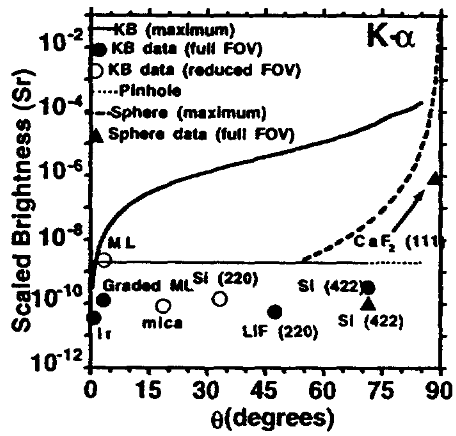

Figure 1 Estimated image brightness for several choices of two-dimensional imaging microscope configurations using the Mn K-α line.

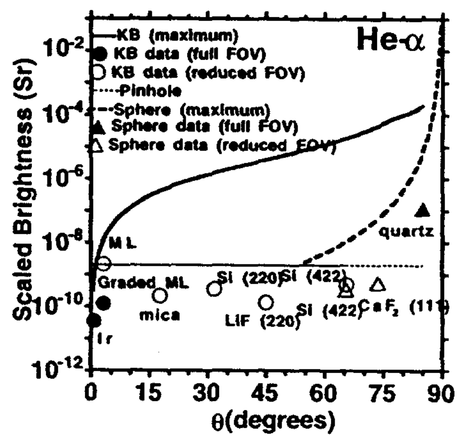

Figure 2 Estimated image brightness for several choices of two-dimensional imaging microscope configurations using the Mn He-α line.

It is clear in principle from Figs. 1 and 2 that for the 2-dimensional imaging cases we consider here, spherical crystals operating within ~ 5 - 10 degrees of normal incidence meet the requirements for source resolution over a specified FOV while providing the highest image brightness. This is because the geometrical optics-limited collection angle is relatively large near normal incidence, because chromatic vignetting of the collection angle is less important near normal incidence, and because there is only one reduction in image brightness for crystal efficiency. However, the general utility of near-normal incidence spherical or toroidal crystals for high energy x-ray imaging at NIF and similar future facilities will depend on two main factors. The first is the limited choice of operating wavelengths, dictated by the requirement that θ be near 90 degrees and by the limited number of useful crystal planes. We have begun a systematic search for matches between desirable source emission lines and crystal planes, and further research will be required in order to determine the actual 2d spacings and integrated reflectivities for these crystals while bent to spherical or toroidal shapes.

The second limiting factor for spherical crystal imaging is crystal quality. For high resolution imaging applications, crystal perfection must be high, since mosaic structure will result in degraded spatial resolution. Additionally, the mechanical properties of bent crystals are also important, as the crystals must maintain their high perfection while bent to spherical or toroidal shapes. Further research is required in order to assess these issues for specific crystal choices.

For the parameters considered, a KB using conventional multi-layer mirrors is more efficient than one using depth-graded multi-layer mirrors. This is because the band-width of the conventional multi-layer mirror is sufficient to avoid chromatic vignetting of the collection angle, and the larger band-width of the graded mirror is unnecessary for increasing the image brightness. The peak reflectivity of the depth-graded mirror is reduced by a factor of ~ 4, however, accounting for the factor of ~ 16 decrease in image brightness compared with the conventional multi-layer mirror. The bent-crystal KB systems all suffer from low integrated reflectivity compared with multi-layer mirrors, so that the increased geometrical solid angles achievable at larger θ are more than offset by decreased efficiency. Because of its two efficiency losses, a KB using Si 422 crystals provides only a slight increase in image brightness over a single off-normal Si 422 spherical crystal, and this implies that bending crystals to toroidal shapes may be a more efficient means of increasing image brightness than the use of dual-crystal arrangements [10].

It is also clear from Figs. 1 and 2 that in many cases, the specified 2 mm field of view cannot be achieved with bent-crystal KB systems or with conventional multi-layer-coated mirrors. This is due to chromatic vignetting of the field of view caused by finite source line-widths and mirror band-widths, and is particularly significant with the narrow-band He-α source . This obstacle to further Bragg-reflector microscope development could be avoided by introducing apertures on the detector side of the mirrors, as illustrated in Fig. 3. Here, the aperture is placed along the chief on-axis reflected ray at a distance $x = 2f$ from the mirror, where $f = Mp/(M+1)$. The aperture width limits the collection angle, while the mirror dimension limits the field of view rather than the collection angle. The aperture technique described here does not require a backlight source on the Rowland circle and does not place any limitations on backlight dimensions, and in addition can be used for emission imaging. However, further research is required in order to determine the geometrical limitations to the aperture width and thus the collection angle for this geometry.

We gratefully acknowledge the contributions and support of M. Cable, G. Collins, U. Feldman, J. Kilkenny, and B. Remington. This work was performed under the auspices of the U.S. Department of Energy by the Lawrence Livermore National Laboratory under contract No. W-7405-ENG-48.

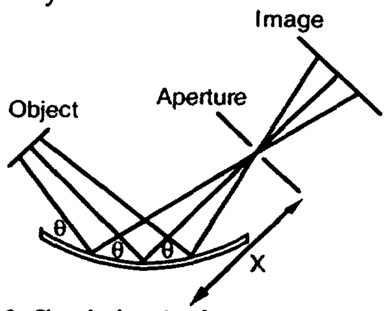

Figure 3. Sketch showing how an aperture, placed behind a mirror on the Rowland circle, can be used to minimize chromatic vignetting of the field of view with Bragg-reflector mirrors.

REFERENCES

1. J. Lindl, Phys. Plasmas **2**, 3933 (1995).
2. F. J. Marshall and Q. Su, Rev. Sci. Instrum. **66**, 725 (1995).
3. C. Brown et al., Rev. Sci. Instrum. **68**, 1099 (1997).
4. M. Dirksmöller et al., Opt. Comm. **118**, 379 (1995).
5. J. A. Koch et al. (submitted for publication).
6. J. F. Seely et al., Appl. Opt. **35**, 4408 (1996).
7. H. T. Yamada et al., Lawrence Berkeley Laboratory Report No. LBL-22800 (1986).
8. B. L. Henke et al., Atomic Data and Nuc. Tables **54**(2) (1993).
9. N. G. Alexandropolous et al., Appl. Spectrosc. **28**, 155 (1974).
10. E. Förster et al., Exp. Tech. Physics **42**, 19 (1996).

***Technical Information Department* • Lawrence Livermore National Laboratory**
University of California • Livermore, California 94551